The PI Controller Research of UPQC in Micro-grid Based on RBF Neural Network

Fuyin Ni[1,2], Zhengming Li[*,1]

[1]*School of Electrical and Information Engineering*, Jiangsu University, Jiangsu, Zhengjiang, 212013, China
[2]*School of Electrical and Information Engineering*, Jiangsu University of Technology, Jiangsu, Changzhou, 213001, China

Abstract **— Aiming at the micro-grid deteriorating the distributed network power quality for its features like voltage fluctuation and intermittent, unified power quality conditioner (UPQC) is the most effective device for power quality treatment. The voltage sag detection of UPQC based on PI with RBF (Radial Basis Function) neural network controller is put forward in the paper. The UPQC topology which includes photovoltaic array is constituted. The PI control strategy based on RBF neural network is studied, and algorithm steps are summarized. After that the compensation instruction controlled by presented PI controller is used to modulate pulse width, and the pulses drive universal bridge to compensate voltage. The simulations show that the proposed PI controller has a better voltage compensation effect than the traditional PI controller through simulation comparison. It can detect voltage sag quickly and improve the micro-grid power quality. The new control strategy has strong anti-jamming capacity and robustness. It provides a new control strategy for UPQC treating power quality of micro-grid.**

Keywords — unified power quality conditioner, RBF neural network, micro-grid, series active power filter, PI controller

I. INTRODUCTION

With the modern technology development and new industry rise, micro-grid has been applied widely in the production and life. Especially, photovoltaic generation and wind generation is got development fast. Both of them have the features such as voltage fluctuation and intermittent, and deteriorate the power quality with increase of micro-grid permeability [1, 2]. The voltage fluctuation is a prominent problem among power quality problems. The transient state power quality problems like voltage fluctuation have caused more and more accidents, which include computer system turbulence, adjusting-speed equipment tripping, mechanical and electrical equipment malfunction, etc. Then the accidents lead to much industrial loss and personal security.

Unified power quality conditioner (UPQC) is a comprehensive power quality treatment device that is made up of series active power filter (SAPF) and parallel active power filter (PAPF) [3]. The UPQC operating principle is that SAPF compensates voltage fluctuations and PAPF compensates harmonic current. The UPQC is becoming hot research issue and has vast potential for future development in the field of power quality treatment [4-8].

Currently, aiming at voltage fluctuation detection of UPQC series side, some main methods are listed as below [9-12]. (1) $\alpha\beta 0$ transformation method based on instantaneous reactive power theory. (2) $dq0$ transformation method based on instantaneous reactive power theory. In reference [9], instantaneous reactive power theory detection method is used for simulation of voltage fluctuations and calculation of short-time flicker value. (3) Wavelet analysis method. Reference [12] proposes recognition of transient power quality disturbances
based on CWD spectral kurtosis. Usually, the computation burden of wavelet transformation method is too much and leads to poor real-time performance, which is key factor to the application of wavelet transformation.

Considering to overcoming the shortage of relative references, the voltage sag detection of UPQC series side based on PI with RBF (Radial Basis Function) neural network controller is put forward according to $dq0$ theory. The UPQC topology which include photovoltaic array is constituted in the paper. The PI control strategy based on RBF neural network is studied. After that the compensation instruction controlled by presented PI controller is used to modulate pulse width. Therefore the output compensation voltage can track the signal of voltage compensation instruction to keep load voltage stability.

II. UPQC SAPF CONTROL SCHEME

The proposed UPQC topology structure is described in Fig. (1). The power system is three-phase three-wire structure, and U_s is three phase voltage resource, and load is nonlinear loads. SAPF and PAPF are connected by DC capacitor. Besides, the boost electric circuit is also connected to UPQC DC side. The photovoltaic array can generate power to loads once the power grid failures.

*Address correspondence to this author at the School of Electrical and Information Engineering, Jiangsu University, Jiangsu Zhengjiang, 212013, P.R. China; E-mail: lzming@ujs.edu.cn

DOI 10.5013/IJSSST.a.17.28.02 ISSN: 1473-804x online, 1473-8031 print

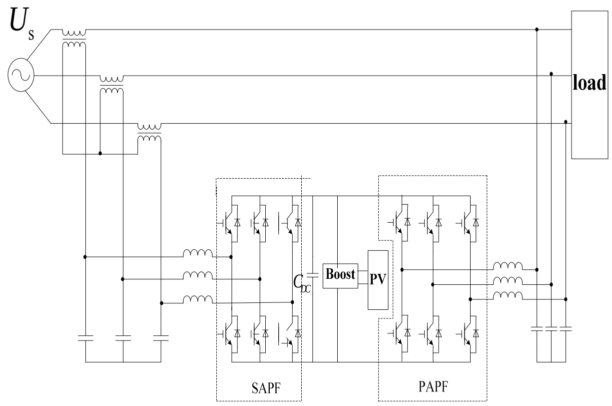

Fig.1 UPQC topology structure

As is shown in Fig. 1, the SAPF in topology structure is mainly used to compensate voltage sag. The SAPF control block is presented in Fig. (2).

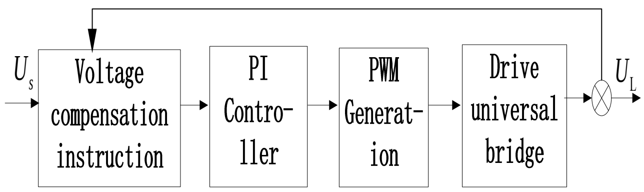

Fig.2 SAPF of UPQC control block

In Fig.(2), the input variable is grid resource U_s , the voltage compensation instruction is got by the voltage detection method of $dq0$ based on instantaneous reactive power theory. For RBF neural network has features of optimum approach and global optimum that other neural network hasn't [13]. What's more, its structure is simple and calculating speed is fast. So the PI controller based on RBF neural network is adapt to generate PWM (pulse width modulation) and drive universal bridge, which can compensate voltage sag fast and perfectly.

III. VOLTAGE SAG DETECTION METHODS BASE ON $dq0$

The voltage sag detection method of UPQC series side block based on $dq0$ is shown in Fig.3.

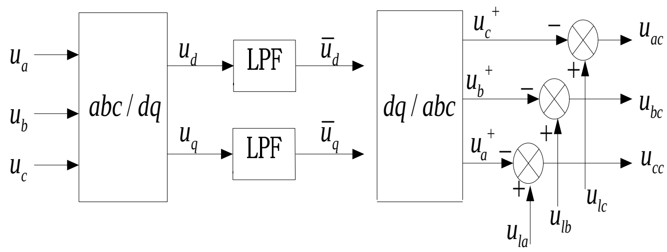

Fig.3 Voltage sag detection method based on $dq0$

In Fig.(3), three-phase grid voltage expression is shown in Equ.(1):

$$\begin{cases} u_a = u_a^+ + u_a^- + u_0 + \sum_{n=2}^{\infty}\left(u_{an}^+ + u_{am}^-\right) \\ u_b = u_b^+ + u_b^- + u_0 + \sum_{n=2}^{\infty}\left(u_{bn}^+ + u_{bm}^-\right) \\ u_c = u_c^+ + u_c^- + u_0 + \sum_{n=2}^{\infty}\left(u_{cn}^+ + u_{cm}^-\right) \end{cases} \quad (1)$$

Where, u_a, u_b, u_c is three-phase grid voltage, u_a^+, u_b^+, u_c^+ is three-phase positive-sequence component, u_a^-, u_b^-, u_c^- is three-phase negative sequence component. u_0 is zero-sequence component, $u_{an}^+, u_{bn}^+, u_{cn}^+$ is n-order harmonic positive-sequence component. $u_{an}^-, u_{bn}^-, u_{cn}^-$ is n-order harmonic positive-sequence component.

The three-phase transformation formula from u_{abc} to u_{dq0} is presented in Equ. (2)

$$u_{dq0} = Cu_{abc} \quad (2)$$

Where, $u_{dq0} = \left[u_d\ u_q\ u_0\right]^T$, $u_{abc} = \left[u_a\ u_b\ u_c\right]^T$, and C is Park transformation matrix. C expression is in Equ. (3)

$$C = \sqrt{\frac{2}{3}} \begin{bmatrix} \cos\omega t & \cos\left(\omega t - \frac{2}{3}\pi\right) & \cos\left(\omega t + \frac{2}{3}\pi\right) \\ -\sin\omega t & -\sin\left(\omega t - \frac{2}{3}\pi\right) & -\sin\left(\omega t - \frac{2}{3}\pi\right) \\ \frac{1}{\sqrt{2}} & \frac{1}{\sqrt{2}} & \frac{1}{\sqrt{2}} \end{bmatrix} \quad (3)$$

The direction component $\begin{bmatrix} \overline{u_d} \\ \overline{u_q} \end{bmatrix}$ is obtained by filtering higher harmonic according to Fig. 3.

$$\begin{bmatrix} \overline{u_d} \\ \overline{u_q} \end{bmatrix} = \sqrt{\frac{2}{3}} U^+ \begin{bmatrix} \cos(\varphi^+) \\ \sin(\varphi^+) \end{bmatrix}$$

Where, U^+ is fundamental harmonic positive-sequence phase voltage actual amplitude, ϕ^+ is fundamental harmonic positive-sequence initial phase.

The fundamental harmonic voltage positive-sequence u_a^+, u_b^+, u_c^+ is got by Equ. (4)

$$\begin{bmatrix} u_a^+ \\ u_b^+ \\ u_c^+ \end{bmatrix} = C^{-1} \begin{bmatrix} \overline{u_d} \\ \overline{u_q} \end{bmatrix} = \begin{bmatrix} U^+ \cos(\omega t + \varphi^+) \\ U^+ \cos(\omega t - \frac{2\pi}{3} + \varphi^+) \\ U^+ \cos(\omega t + \frac{2\pi}{3} + \varphi^+) \end{bmatrix} \quad (4)$$

U_{la}, U_{lb}, U_{lc} is three-phase loads voltage. Then the distorted voltage is shown in Equ. (5)

$$\begin{cases} u_{ac} = u_{la} - u_a^+ \\ u_{bc} = u_{lb} - u_b^+ \\ u_{cc} = u_{lc} - u_c^+ \end{cases} \quad (5)$$

Where, u_{ac} , u_{bc} , u_{cc} is UPQC series side voltage compensation instruction. After that, PWM is got by PI controller in accordance with the instruction from Fig. 2. Lastly, PWM signal drives three-phase IGBT module to realize voltage compensation.

IV. PI CONTROL STRATEGY BASED ON RBF NEURAL NETWORK

A. RBF Neural Network Model

RBF neural network is three-layer feed-forward network with single hidden layer. The mapping from input to output is nonlinear, but the mapping from hidden layer space to output space is linear. RBF neural network accelerates the learning speed and avoids local minimum problem. So it is well applied to control engineering [14-15]. Its structure is described in Fig. (4). It is made up of one input layer, one hidden layer and one output layer.

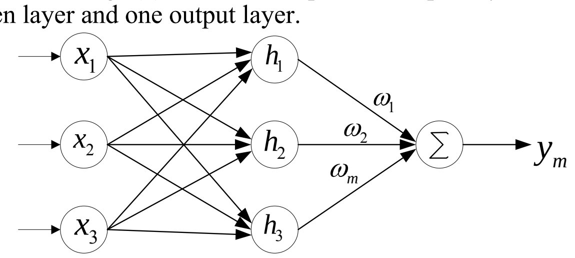

Fig. 4. RBF neural network structure

In Fig.4, $x = [x_1, x_2, ..., x_n]^T$ is input vector. $h = [h_1, h_2, ..., h_m]^T$ is radial basis vector, and h_j is Gause basis function, it is expressed in Equ. (6)

$$h_j = \exp\left(-\frac{\| x - c_j^2 \|}{2b_j^2}\right), j = 1, 2, ...m \quad (6)$$

Where, j is the core vector of node. C_j is node core vector, $C_j = \left[c_{j1}, c_{j2} ... c_{ji} ... c_{jn}\right]^{\mathrm{T}}, i = 1, 2, ..., n$, and its parameter is as below

$$\Delta c_{ji}(k) = \eta\left(y(k) - y_m(k)\right) w_j \frac{x_j - c_{ji}}{b_j^2} \quad (7)$$

$$c_{ji}(k) = c_{ji}(k-1) + \Delta c_{ji}(k) + \alpha\left(c_{ji}(k-1) - c_{ji}(k-2)\right) \quad (8)$$

$B = [b_1, b_2, ..., b_m]^{\mathrm{T}}$ is neural network basis width vector. b_j is basis width parameter of the j node, and basis width parameter is as below

$$\Delta b_j(k) = \eta\left(y(k) - y_m(k)\right) w_i h_j \frac{\| X - C_j \|^2}{b_j^3} \quad (9)$$

$$b_j(k) = b_j(k-1) + \Delta b_j + \alpha\left(b_j(k-1) - b_j(k-2)\right) \quad (10)$$

$W = \left[[w_1, w_2, ..., w_m]\right]^{\mathrm{T}}$ is weight vector, according to gradient descent algorithm, the output weight vector parameter is as below

$$\Delta w_j(k) = \eta\left(y(k) - y_m(k)\right) h_j \quad (11)$$

$$w_j(k) = w_j(k-1) + \Delta w_j(k) + \alpha\left(w_j(k-1) - w_j(k-2)\right) \quad (12)$$

Where, η is learning speed, α is factor of momentum.

The identified network output is

$$y_m(k) = w_1 h_1 + w_2 h_2 + ... + w_m h_m \quad (13)$$

The indictor function of identifier feature is

$$J = \frac{1}{2}\left(y(k) - y_m(k)\right)^2 \quad (14)$$

Then Jacobian matrix is defined as

$$\frac{\partial y(k)}{\partial \Delta u(k)} = \frac{\partial y_m(k)}{\partial \Delta u(k)} = \sum_{j=1}^{m} w_j h_j \frac{c_{ji} - x_1}{b_j^2} \quad (15)$$

Where, $x_1 = \Delta u(k)$.

B. PI Control Strategy Based on RBF Neural Network

The principle of PI based on RBF neural network controller is illustrated in Fig. (5), it is integrated advantages of RBF neural network algorithm and PI algorithm. In Fig. 5, input variable y_{d} refers to u_{ac}, u_{bc}, u_{cc} , output variable y refers to u_{ref} which controls PWM.

The two parameters of PI controller are self-adjusted in the RBF neural network. Firstly, the gradient information is got by the neural network online identifier. PI parameters are on-line adjusted for adapting to parameters variation according to the information, which makes PWM more accurate.

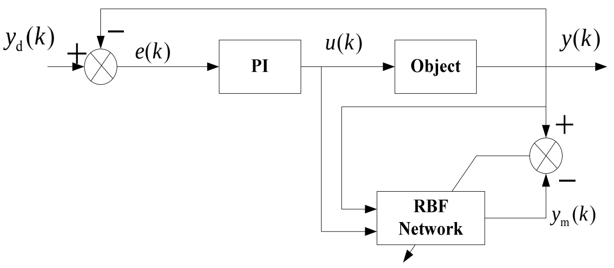

Fig.5 Principle of PI based on RBF neural network controller

To the incremental PI controller, its algorithm is:

$$u(k)=u(k-1)+\Delta u(k) \tag{16}$$

$$\Delta u(k)=k_p\left(e(k)-e(k-1)\right)+k_i e(k) \tag{17}$$

In according with the RBF algorithm, the neural network indictor is

$$E(k)=\frac{1}{2}e(k)^2 \tag{18}$$

The adjusting of k_p, k_i is acquired by gradient descent method

$$\Delta k_p=-\eta\frac{\partial E}{\partial k_p}=-\eta\frac{\partial E}{\partial y}\frac{\partial y}{\partial \Delta u}\frac{\partial \Delta u}{\partial k_p}=\eta e(k)\frac{\partial y}{\partial \Delta u}xc(1) \tag{19}$$

$$\Delta k_i=-\eta\frac{\partial E}{\partial k_i}=-\eta\frac{\partial E}{\partial y}\frac{\partial y}{\partial \Delta u}\frac{\partial \Delta u}{\partial k_i}=\eta e(k)\frac{\partial y}{\partial \Delta u}xc(2) \tag{20}$$

Where, $\frac{\partial y}{\partial \Delta u}$ is Jacobian information of control object, which is identified by neural network.

Summing up the PI controller based on RBF neural network algorithm is as below:

(1) Initialize neural network parameters such as node number, core vector, basis width, PI parameter initial value, learning speed.

(2) Calculate error, $e(k)=y_d(k)-y(k)$.

(3) Constructor RBF neural network by gradient descent method, and adjust network parameters by online learning algorithm.

(4) Adjust PI controller k_p, k_i according Equ. (19), (20).

(5) Calculate output $u(k)$ by incremental PI control algorithm;

(6) Return to Step (2), sample and control next time.

Therefore PI controller parameters k_p, k_i can be got through online adjusting. Then the compensation instruction controlled by PI controller generates PWM signal.

V. SIMULATION AND ANALYZATION

The UPQC series side simulation model in the photovoltaic micro-grid is established by Simulink according to new topology structure. The general simulation model is

shown in Fig. (6). PV1 module supplies DC power for SAPF and PAFP. PV2 module is connected to grid in parallel. The three-phase breaker is set to control open or cutoff the SAPF at load side.

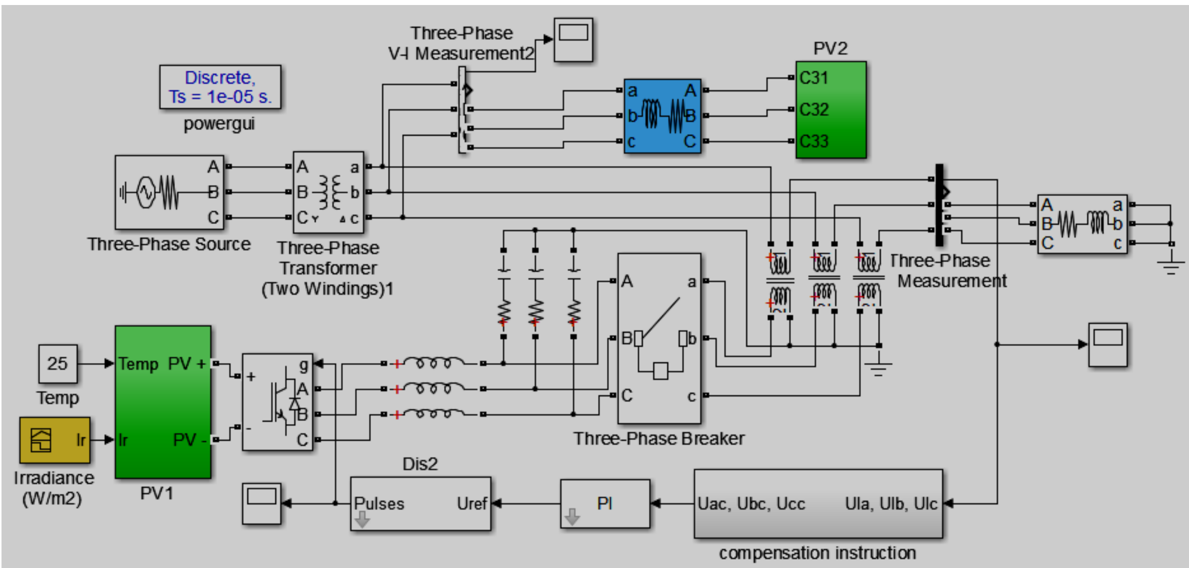

Fig.6 UQPC series side in the Photovoltaic micro-grid simulation model

DOI 10.5013/IJSSST.a.17.28.02 ISSN: 1473-804x online, 1473-8031 print

The SAPF parameters are set in TABLE I.

TABLE I. SAPF PARAMETER

Parameters	Value
Three-phase transformer1	10000:380
Transformer 2	3:1
PV array temperature	25□
Light intensity	1000W/m^2
cell quantity of PV1 module	100 pieces
cell quantity of PV2 module	40 pieces
cell power	250W
SAPF DC side voltage	500V
capacity of DC side	750μF/600V
filtering capacity C	4.7uF/460V
filtering capacity R	2Ω
filtering capacity L	5.6mH
Load (R, L)	1000Ω, 2mH

Sample period is set to be 0.1us. The initial values of PI with RBF neural network controller in the UPQC series side is set in TABLE II.

TABLE II. THE INITIAL VALUES OF PI CONTROLLER BASED ON RBF NUERAL NETWORKING

Parameters	Value
input vector	[2, -2, 3]
core vector	[-1, 1, 2; 3, 0, 2]
basis width vector	[1, 1, 1]
weight vector	[2, 3, 2]
PI parameter	0.15
PI parameter	3
learning speed	0.25
factor of momentum	0.04

Set the voltage generated by PV2 module to drop at t=0.15s, as is shown in Fig. (7a), voltage waveform begins to decline at t=0.15s. And set the three-phase breaker close at 0.25s. Then the SAPF based on PI with RBF neural network contoller is operated immediately at t=0.25s. Therefore the load voltage waveform is restored as orignal. The compensated voltage waveform is very smooth and stable from the simulation figure.

Fig. (7b) is load voltage compensation simulation waveform based on tradional PI algorithm. The SAPF also begins to compensate voltage at t=0.25s. Compared to Fig. (7a), the simulation waveform is less smooth and longer response time than compensation waveform by PI with RBF algorithm. It is concluded that the proposed PI controller can get a better compensation effect than the tradional PI controller.

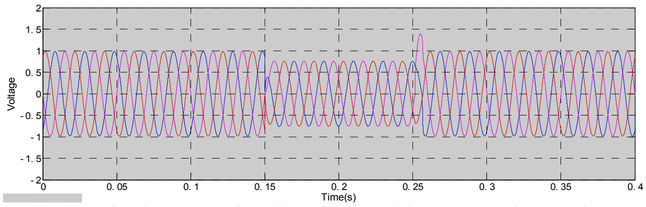

(a) Load voltage waveform based on PI with RBF neuarl network

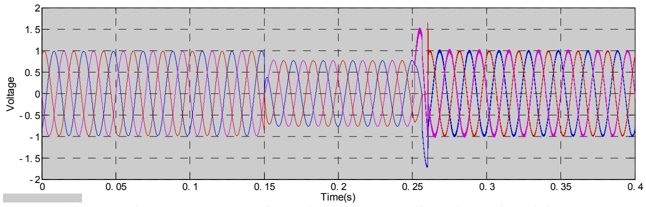

(b) Loads voltage waveform based on tradional PI algorithm

Fig.7 Loads voltage compensation simulation waveform

Both of the two compensation effects are also compared by voltage spectrum. Fig.(8) is described the load voltage spectrum. According to Fig. (8a), the voltage THD is 4.21% based on PI with RBF neural network controller. In Fig. (8b), the voltage spectrum based on traditional PI controller is 14.49%. Obviously, it is manifested that compensation effect based on PI based on RBF neural network is much better than based on traditional PI algorithm.

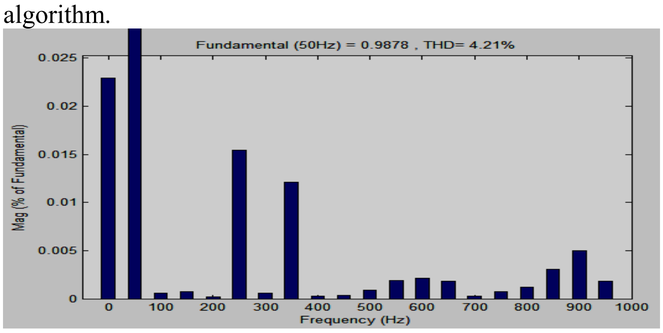

(a) Loads voltage spectrum based on PI with RBF neural network

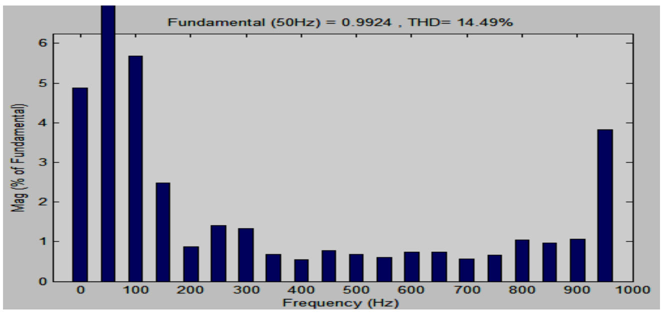

(b) Loads voltage spectrum based on traditional PI

Fig.8 Loads voltage spectrum

VI. CONCLUSION

Aiming at instability and intermittent of micro-grid, the new topology of UPQC is established that the photovoltaic boost circuit supply DC voltage in this paper. The voltage detection method of UPQC series side based on PI with RBF neural network controller is put forward. In the proposed algorithm, the gradient information is got by the neural network online identifier. PI parameters are on-line adjusted for adapting to parameters variation according to the information, which makes PWM more accurate and stable. The simulations show that the proposed PI controller has a better voltage compensation effect than the traditional PI controller through simulation comparison. It provides a new control strategy for UPQC treating the power quality of micro-grid.

CONFLICT OF INTEREST

The author confirms that this article content has no conflict of interest.

ACKNOWLEDGMENT

Supported by National Natural Science Foundation of China（51477070）

Supported by Jiangsu Province Prospective Joint Research Project（BY2015028-01）

Supported by A Project Funded by The Priority Academic Program Development of Jiangsu Higher Education Institutions (PAPD)

REFERENCE

[1] Y. H. Huang, J. J. Xu, Y. K. Sun, "Dynamic voltage restorer in micro-grid based on a minimum energy compensation control scheme," Transactions of China Electrotechnical Society, vol. 29, No.12, pp. 128-136, Dec. 2014.

[2] W. Jiang, W. Chen, R. J. Hu, "United power quality conditioner based on supercapacitor for microgird," Electric Power Automation Equipment, vol. 34, No. 1, pp. 85-90, Jan. 2014.

[3] V. Khadkikar, "Enhancing electric power quality using UPQC: A comprehensive overview," IEEE Transactions on Power Electronics, vol. 27, No. 5, pp. 2284-2297, May. 2012.

[4] B.B. Ambati, V. Khadkikar, "Optimal sizing of UPQC considering VA loading and maximum utilization of power-electronic converters," IEEE Transactions on Power Delivery, vol. 29, No. 3, pp. 1490-1498, 2013,

[5] G.S. Kumar, B.K. Kumar, M.K. Mishar, "Mitigation of voltage sag with phase jumps by UPQC with PSO-based ANFIS," IEEE Transactions on Power Delivery, vol. 26, No. 4, pp. 2761-2773, 2011.

[6] I. Axente, J. N. Ganesh, M. Basu, M. F. Conlon, Gaunghan Kevin, "A 12-kVA DSP-controller laboratory prototype UPQC capable of mitigating unbalance in source voltage and load current," IEEE Transactions on Power Electronics, vol. 25, No. 6, pp. 1471-1479, 2010.

[7] S. B. Karanki, M. K. Mishra, B. K. Kumar, "Particle swarm otimization based feedback controller for unified power quality conditioner," IEEE transaction on Power Delivery, vol. 25, No. 4, pp. 2814-2824, 2010.

[8] Q. N. Trinh, H. H. Lee, "Improvement of unified power quality conditioner performance with enhanced resonant control strategy," Generation Transmission & Distribution, IET, vol. 8, No. 12, pp. 2114-2123, 2014.

[9] J. D. Wang, K. Liu, Y. J. Gao, "Detection for voltage fluctuation and flicker calculation based on the instantaneous reactive power theory," Power System Protection and Control, vol. 40, No. 2, pp. 145-150, 2012.

[10] Z. Q. Liang, H. C. Shu, "Novel UPQC DC voltage research of $PI^{\lambda}D^{\mu}$ Controller," Transactions of China Electrotechnical Society, vol. 25, No. 2, pp. 147-151, 157, 2010.

[11] Y. L. Qin, L. J. Tian, X. F. Chang, " Classification of power quality disturbance based on wavelet energy distribution and neural network," Electric Power Automation Equipment, vol. 29, No. 7, pp. 64-67, 2009.

[12] L. Zhu, Z. G. Liu, Q. L. Hu, Q. G. Zhang, " Recognition of transient power quality disturbances based on CWD spectral kurtosis," Electric Power Automation Equipment, vol. 34, No. 2, pp. 125-131, 2014.

[13] T. Zhang, L. Y. Zhao, X. J. Dang, "Design of hybrid controller based on RBF and PID," Micromotors, vol. 47, No. 12, pp. 48-51, 2014.

[14] J. L. Wang, X. H. Jiao, " Design of PID controller adjusted by RBF neural network for Dfig-based wind farm," AC TA ENERGIAE SOLARIS SINICA, Vol. 32 , No. 3, pp. 311-317, 2011.

[15] Y. M. Pan, W. N. Xue, Q. Z. Zhang, "A forecasting model of RBF neural network based on genetic algorithms optimization," 2011 Seventh International Conference on Natural Computation (ICNC), Vol. 1, pp. 48-51, 2011.